

Simple interferometric setup enabling sub-Fourier-scale ultra-short laser pulses

Enrique G. Neyra^a, Gustavo A. Torchia^a, Pablo Vaveliuk^a, and Fabian Videla^{a,b}

^aCentro de Investigaciones Ópticas (CICBA-CONICET-UNLP), Cno. Parque Centenario y 506, P.O. Box 3, 1897 Gonnet, Argentina

^bDepartamento de Ciencias Básicas, Facultad de Ingeniería UNLP, 1 y 47 La Plata, Argentina

ABSTRACT

In this work, we have developed a method to generate ultra-short pulses below the Fourier limit, extending the concept previously worked in reference 1 for generating sub-diffractive Gaussian beams. Alternatively, we introduce new alternatives based on a temporally non-symmetrical interference to narrow ultrashort pulses allowing, sub-Fourier scales. The experimental setup scheme is simple and versatile being able to work with high-power laser sources and ultra-short pulses with a broad bandwidth at any central wavelength. The results presented, are promising and help to enlighten new routes and strategies in the design of coherent control systems. We glimpse they will become broadly useful in different fields from strong field domain to quantum information.

1. INTRODUCTION

The temporal width of an ultra-short laser pulse $E(t)$, is given by the distribution of the spectral phase $\phi(\omega)$ in the Fourier spectral components of the field $E(\omega)$. The so-called transform-limited pulses condition is full-filled if the spectral phase of the field is independent of the frequency. This condition imply, that the temporal and spectral widths are minimum and in turn, its product correspond to a particular constant in agreement with the pulses shapes. Considering a Gaussian pulse, and their full width at half-maximum (FWHM) temporal and spectral, this product results : $\Delta\omega\Delta t = 2\pi c$ being $c = 0.441$ [2]. Of course, c value changes for other pulse shapes. The Fourier limit is tied to the quantum Heisenberg uncertainty principle since the conjugate variables of both phenomena are related by the Fourier transform. In contrast, if the pulse does not meet this condition, i.e. the spectral phase $\phi(\omega)$ is frequency dependent, so the pulse presents chirp and the FWHM of the pulse is larger than the FWHM of the pulse without chirp. In this sense, on the last years has been emerged interest for a wave phenomenon called superoscillation 3, 4, in which a band-limited function can oscillate faster than their faster Fourier component.

The superoscillatory phenomenon can be seen as an interferometric one, where each spectral component has a particular phase that originate, in the conjugate space, small regions whose FWHMs are below to the Fourier limit. Additionally, those regions where the Fourier limit is "broken", shows a poor efficiency in relation with the initial pulse. In addition, this phenomenon is accompanied with the emerging of side lobes with relative amplitude 1. The superoscillatory phenomenon, is not only an interesting mathematical topic. Several wave phenomena take advantage of superoscillations such as: Focusing different kind of beams for superresolution microscopy 5, in quantum mechanics 6, 7, in acoustic waves 8, in signals 9 and others 4. Additionally, for ultra-short pulses, the Fourier limit can be overcome through devices like the spatial light modulator (SLM) in a pulse shaper prism based 10, which generate the desired phase mask 11–15. However, this experimental setups requires complex process of alignment and control, complemented sometimes with cumbersome numerical tools. It is a customary notion that, the minimum FWHM reachable is associated to a constant spectral phase, but this is not strictly true. The clearest example is put forward by a π -phase mask where sub-Fourier pulses were obtained 13. On the other hand, the ability to manipulate the *shape* of the optical pulses is essential for numerous applications 16 such as spectroscopy and coherent control 17, 18, metrology 19, microscopy 20 and optical communications 21. In this article we propose a robust, versatile and simple method to achieve sub-Fourier ultra-short laser pulses.

Further author information: (Send correspondence to Enrique Neyra)
Enrique Neyra.: E-mail: enriquen@ciop.unlp.edu.ar

The currently approach is inspired in the spatial narrowing of a focused beam recently proposed [1](#). In that work, to print a quadratic phase in the beam spatial profile, a spherical mirror was introduced modifying a branch of a Michelson interferometer. In this work to achieve a quadratic phase in the beam but now in the temporal domain, we replaced the spherical mirror by a water cell (dispersive media) introducing *chirp* on the original pulse, and as result, after the cell, a temporally widened pulse is obtained. To assess the performance of the proposed experimental scheme we developed two experiments. The first one is based on the control of attenuation through a polariser. The second one is based on the control of the delay. Both systems were introduced in the same branch of a Michelson interferometer. These alternatives showed the desired behavior, allowing sub-Fourier scale ultrashort pulses.

2. THEORETICAL FRAMEWORK

In order to mathematically describe the interfering process, we call $E(t)$ the pulse originated as a result of the superposition of *pulse 1* (unaltered pulse) and *pulse 2* (altered pulse) after pass through the interferometric device. The *pulse 1* is a band-limited ultra-short Gaussian pulse $E_0(t)$, with spectral content $E_0(\omega) = E_0 e^{-((\omega-\omega_0)/\delta\omega)^2}$, centered at the carrier frequency ω_0 whose bandwidth is represented by $\delta\omega$. Therefore, the whole field in the frequency domain, composed by the unaltered and the altered pulse is given by

$$E(\omega) = E_0(e^{-\frac{(\omega-\omega_0)^2}{\delta\omega^2}} + \alpha e^{-\frac{(\omega-\omega_0)^2}{\delta\omega^2}} e^{-i\beta(\omega-\omega_0)^2} e^{i\phi}) \quad (1)$$

Clearly, the phase of *pulse 2* is modified by the chirp parameter (β), in turn the amplitude is modified by (α), a factor which weights the relative amplitude between the arms. Besides, there is a third controllable parameter, (ϕ), representing the relative phase between both arms of the interferometer. The Fourier transform of the Eq. (1) returns the narrowing pulse in the time domain

$$E(t) = e^{-\frac{1}{4}t^2} e^{i\omega_0 t} + \frac{\alpha}{(1+\beta^2)^{1/4}} e^{-\frac{1}{4(1+\beta^2)}t^2} e^{i\Phi(t)} e^{i\omega_0 t}, \quad (2)$$

where the t -varying phase is

$$\Phi(t) = \frac{\beta}{4(1+\beta^2)^2} t^2 - \frac{1}{2} \arctan(\beta) - \phi. \quad (3)$$

The Fourier transform was evaluated taken $\delta\omega$ and E_0 equal to the unit, for a sake of clarity to visualize the technique highlights.

Explicitly, Eq. (2) shows the interference between a Fourier-transform-limited pulse $E_0(t) = e^{-\frac{1}{4}t^2}$ and the widened version of this pulse, broadened by the factor $\tau = \sqrt{1+\beta^2}$ with relative amplitude $\alpha/(1+\beta^2)^{1/4}$ and phase $\Phi(t)$.

It is well-known that the chirp quadratic parameter β , in the temporal domain, is originated when the pulse travels through of a dispersive medium. This parameter is related to the group velocity dispersion (GVD) by $\beta = \frac{1}{2}GVD \times L$, where L is the length of the dispersive media [2](#). The pulse intensity $I(t)$ is then obtained by multiplying Eq.2 by its complex conjugate to give:

$$I(t) = e^{-\frac{1}{2}t^2} + \frac{\alpha^2}{\sqrt{1+\beta^2}} e^{-\frac{t^2}{2(1+\beta^2)}} + \frac{2\alpha}{4(1+\beta^2)^{1/4}} \cos \Phi \quad (4)$$

Equation (4) represents the temporal intensity profile of the field $E(t)$, that for a suitable choice of the external parameters β , α and ϕ , make it possible to conform a pulse whose central lobe shows a temporal width below the Fourier limit, i.e. narrower than the reference pulse $E_0(t)$. For this purpose, it is necessary a pure destructive interference condition between the pulses, that is achieved for values of the phase $\phi = \phi(\alpha, \beta)$, α and β . A complete theoretical description of this interference was done in Ref [1](#), for the spatial domain, but despite of the different domains, this process can be seen as equivalent.

3. EXPERIMENTAL

3.1 Setup

The experimental setup used to carry out the proposed approach to synthesize narrower pulses is sketched in Fig. 1.

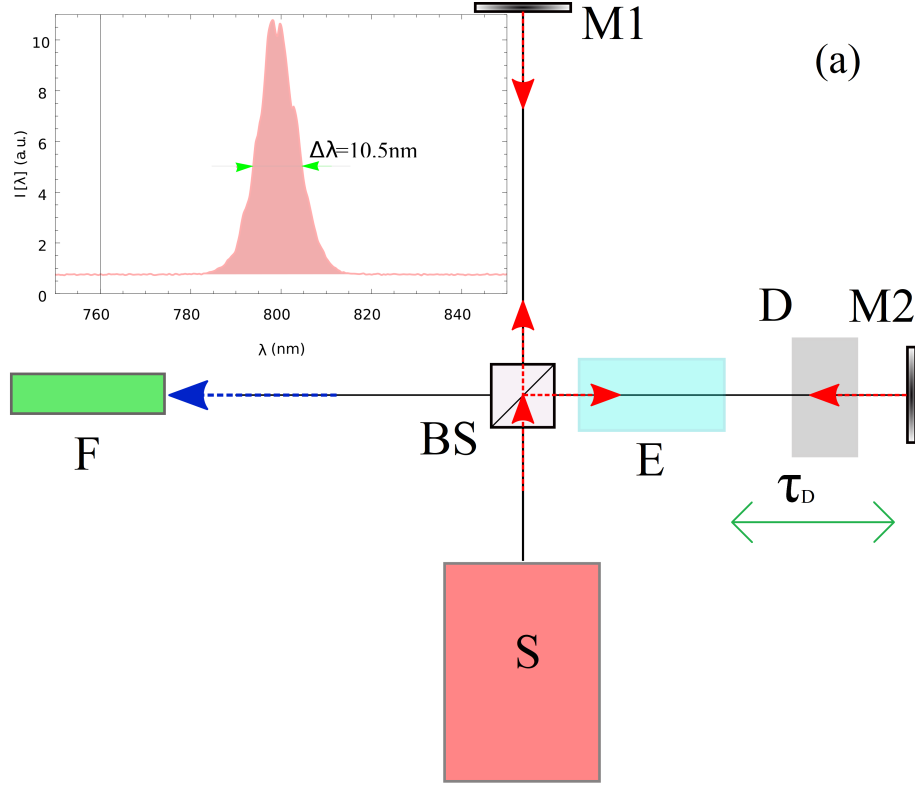


Figure 1. Our experimental setup for synthesise pulses is based on a Michelson Interferometer (MI).

S is the femtosecond laser source, a Ti:Sapphire femtosecond oscillator. M1 and M2 are the fixed and mobile mirrors respectively. BS is the beam splitter. In the delay line, the water cell E (dispersive medium) is followed by a half-wave plate (HWP) plus a polarizer, D, at the opposite end, the GRENOUILLE system F

Input ultrashort pulse enters into a Michelson Interferometer (MI), then it is splitting in two pulses by mean of a beam-splitter (BS). The *pulse 1* travels through the branch 1 of the interferometer and then is reflected by the fixed mirror (M1), remaining unaltered. The *pulse 2* travels through the branch 2, this arm corresponds to the action of the different control parameters, α , β and ϕ . Mirror (M2) is mounted in a micro-meter translation stage and controls the relative phase ϕ between the interferometer arms. During the first experiment, MI is setting as a balanced interferometer, while for the second a delay line τ_D is activated to accomplish a non-symmetrical interference. Besides in branch 2, *pulse 2* is stretched by passing through a water cell of 6 cm long, due to the group velocity dispersion (β parameter, GVD). Cell path is indicated as device E in Fig. 1. In the same branch, the *pulse 2* pass through a half-wave plate (HWP) and a polarizer (P) system to control the relative intensity between both pulses (α parameter), device D in Fig. 1. Finally, when the two pulses are reflected by the mirrors (the pulse cross again the water cell), the resulting interference is detected by a GRENOUILLE system 22, F, that characterise the temporal profile of the pulse synthesis. The laser system employed to test our experimental approach was a Ti:Sapphire femtosecond oscillator (S), Mai Tai model from Spectra Physics (USA), characterised by a spectral bandwidth of 10:5nm, that corresponds to a band-limited pulse of FWHM ≈ 90 fs (see inset of Fig. 1).

3.2 Results and discussions

First of all and for testing, we measured the different pulses widths. The results, were represented in Figure 2. Panel (a) shows the FROG trace for the pulse into branch 1 while Figure 2(b) shows the temporal intensity profile and its phase retrieved by the FROG trace being its temporal width of FWHM=89.8fs. Panel (c) of Figure 2 shows the measured FROG trace corresponding to the stretched pulse by propagation through the water cell (branch 2). Panel (d) presents the FROG retrieved temporal intensity and phase profile of the pulse.

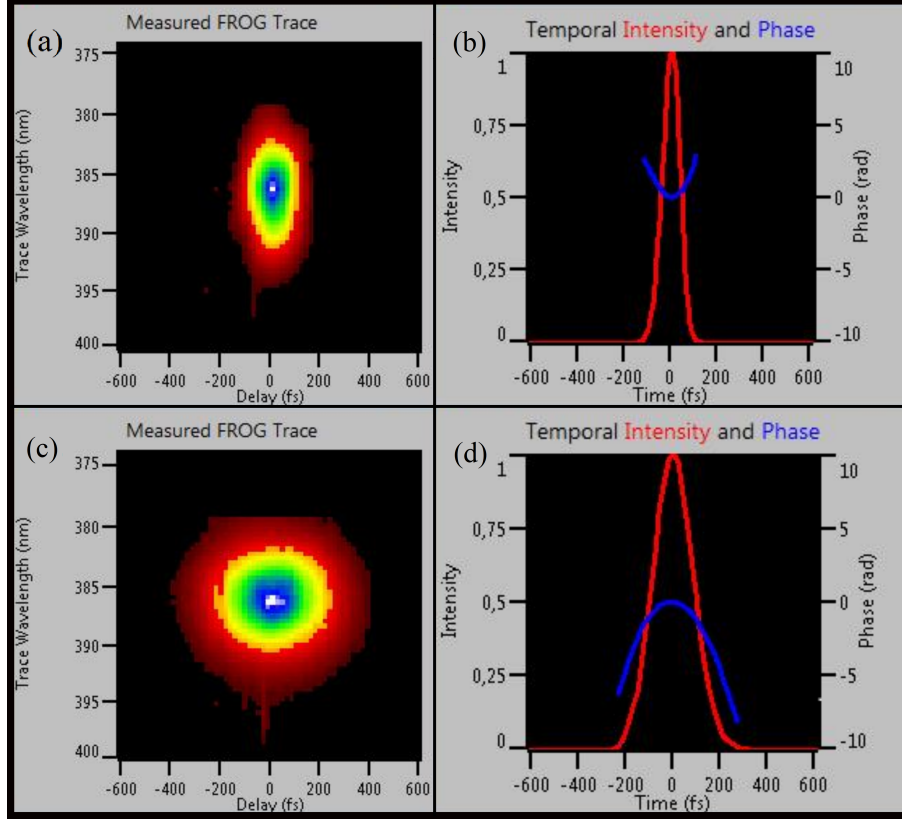


Figure 2. FROG traces corresponding to pulses traveling in each arm of the Michelson Interferometer (left side). Retrieved temporal profiles for the pulses in each arm of the MI. (right side).

It can be observed a FWHM of 199,4fs. By setting properly units and considering $\delta\omega = 1$ it can be obtained the relationship between the FWHMs of the pulses in each branch is $\sqrt{1 + \beta^2}$ (see Eq.3), in this way we can calculate the β value from $\frac{199.4fs}{89.8fs} = \sqrt{1 + \beta^2}$ as $\beta = 1.99$.

Fig 3 present the synthesized pulses experimentally obtained with the interferometric technique described previously. The different pulses widths showed in panels (b) and (d) have been obtained by varying the α parameter handling a half-wave plate plus a polarizer system, detailed in the experimental procedure. In figure 3, panels (a) and (b) show the FROG trace and its retrieved pulse profile, respectively. The result of the interference was measured by setting $\alpha = 0.25$. The FWHM retrieved was 84 fs that corresponds to a reduction of the Fourier limit of 7 percent respect to the input pulse. On the other hand, in Figures 2(c) and 2(d), it is shown the second set of measurements. In this case, the interference pulse was conducted by setting $\alpha = 0.38$. The resultant FWHM was 79 fs, corresponding to a reduction of 12% of the Fourier limited original pulse.

Complementary, Fig 3 (e) shows the evolution of the FWHM corresponding to the central lobe for the synthesised pulse as a function of the α parameter (solid line). FWHM scale was graduated referred to the temporal FWHM of the input pulse. In this simulation, described by equation (4), was considered a fixed value of the β parameter equal to 1.99. A first region from $\alpha=1$ to $\alpha=0.8$, shows a linear relation between FWHM and α . A second region, for $\alpha > 1$, presents a fast reduction of the FWHM. By calculation of equation (4), for

large values of α , the synthesised pulse shows side-lobes with larger amplitude compared to the central lobe, also when the FWHM is close to zero value. As it is described in 23, each side-lobe have different spectral content.

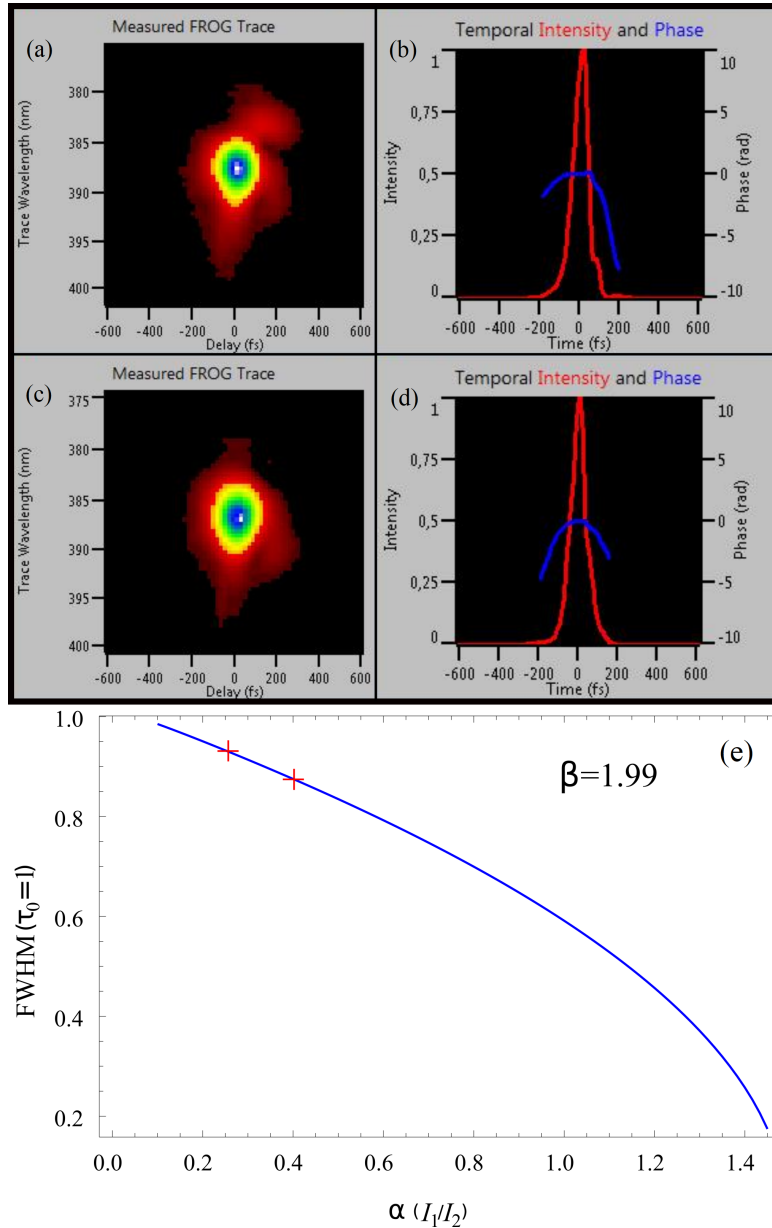


Figure 3. Evolution of FWHM of the synthesised pulses vs α (the amplitude ratio of the interfering pulses). β chirp parameter was held constant at 1.99. The two red crosses correspond to the measured experimental data.

A complete theoretical analysis can be found in Ref. 1. Additionally in Figure 3, experimental points have been indicated by red crosses. In this case, it is important to mention that we could not make measures for large values of α , to verify the theoretical curve (Fig 2(e)), because of technical limitations of the GRENOUILLE system. When measures are made with large values of α , interference rings are generated in the wave-front of the synthesised pulse. We thought that it is because of the additional divergence the pulse experiments when crossing the water cell. It is necessary to work with Gaussian or continuous wave-fronts to achieve a properly operation of the GRENOUILLE system 22.

Alternatively to attenuation control we propose other way to produce similar sub-Fourier synthesized pulses

controlling the delay times by using the same Michelson interferometer. In this case, the method is based on a non-symmetrical interference in the time domain. As we show, Eq.(2) represents the interference between an ultra-short and a widened pulse centred in $t = 0$, which produce a synthesised pulse with sub-Fourier characteristics. The proposed alternative can be achieved if the two pulses travelling in each arm of the MI, the original and widened pulse, have a delay time τ_D when interfere. We will show that changes on the delay produce similar behaviour that changes in the α parameter. Both lead to sub-Fourier pulses.

In Fig. 4 are presented two measurements corresponding to different delay times (τ_D) (see Fig. 1), considered as the distance between peaks of the original and widened pulses respectively (see fig 4).

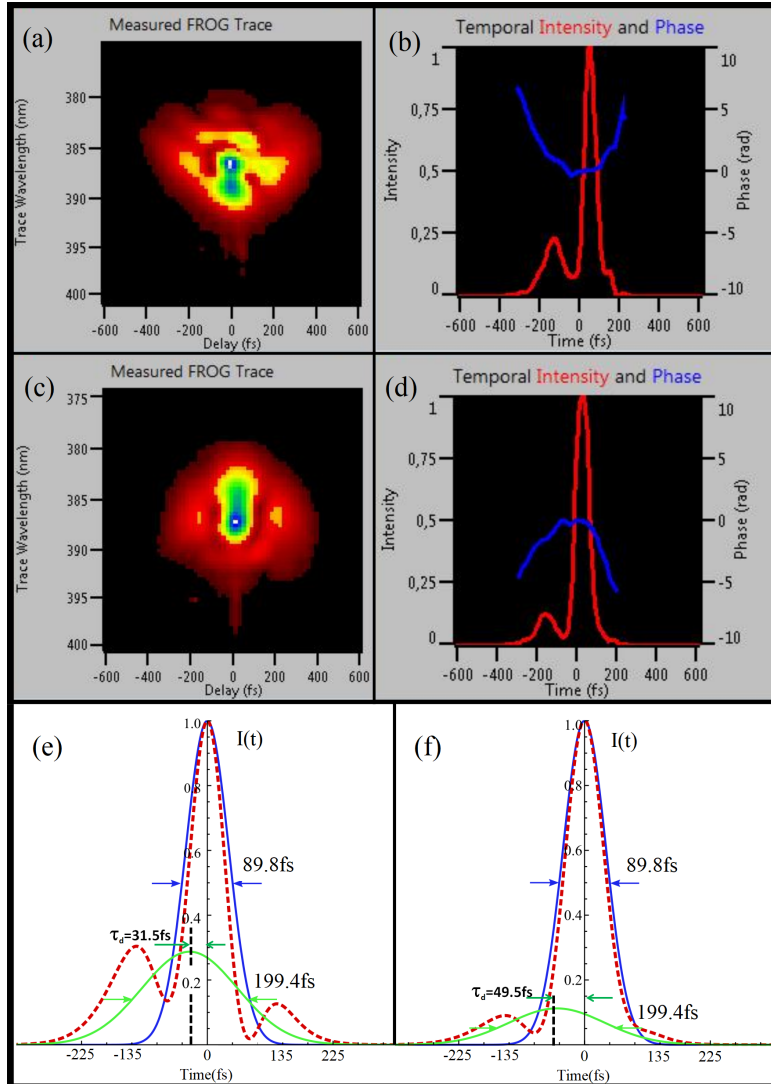


Figure 4. Frog traces corresponding to synthesised pulses for delays of 31.5 fs and 49.5 fs are sketched in panels (a) and (c), respectively. In panels (b) and (d) the temporal counterpart of (a) and (c) respectively. On the bottom panels (e) and (f), detailed for each delay, the resultants pulses (red dashed line). In blue solid and green solid lines, the pulses traveling through branches 1 and 2

The chosen values are : $\tau_D = 31.5\text{fs}$ and $\tau_D = 49.5\text{fs}$ (with $\alpha = 0.85$ and $\alpha = 0.5$ respectively), top and bottom figures, respectively. In fig. 4 panels (a) and (b) at the top, are shown the FROG trace and the retrieved temporal profile corresponding to a delay times of 31.5fs and $\alpha = 0.85$, the synthesised pulse retrieved has a FWHM=68fs (24% of the Fourier limit reduction). In the middle of fig. 4. panels (c) and (d) respectively are

shown the FROG trace and the retrieved temporal profile corresponding to a delay of 49.5fs and $\alpha = 0.5$ giving a resultant pulse with a FWHM=81fs (10% Fourier limit reduction). At the bottom of figure 4, panels (e) and (f) can be seen the respective simulations of the measurements.

The blue line shows the original pulse and in green the widened pulse, with the delay τ_D . In red dashed, is shown the synthesised pulse after the interference, where can be seen the asymmetric distribution of the two side-lobes in agreement with the experimental measurements.

This last alternative to obtain sub-Fourier pulses allows to modulate the temporal width of the pulse as a function of the temporal delay τ_D , this process of FWHM modulation can be described through the next sequence: suppose we began with two pulses temporally spaced by a large delay τ_D which is progressively reduced through the movement of the micro-positioning stage. After that, the Fourier limited pulse will experience a reduction of FWHM. The minimum FWHM is reached when occurs a maximum of destructive interference condition. If τ_D is reduced yet more, the Fourier limited pulse will began to increase again. Depending on the FWHM of the widened pulse, this process is repeated once, twice or n times. In consequence, the temporal width of the initial pulse, will experience a sinusoidal variation with the τ_D parameter.

4. CONCLUSIONS

In conclusion, we have presented two simple approaches, supported by experimental results, to obtain ultra-short pulses where its FWHMs are below the Fourier limit. This technique, based on an interferometric process, shows some advantage in relation to the previous ones, commonly used for this purpose, such as the capability to work with high power laser sources and operate with ultra-bandwidth pulses centered at any wavelength, limitations can be associated with different devices employed: beam-splitter, mirrors, etc. which are affected by thermal fluctuations, mechanical vibrations, fluence threshold of mirrors, etc. this is intrinsic properties of a Michelson interferometer. Alternatively in our experimental setup, the aberrations are negligible, because of the use of passive devices, while a pulse shaper implemented with an SLM presents aberrations given by the pixel size 14. We think, that this new strategy for pulse synthesis could open a new route to address ultra-fast spectroscopy, as well as a different coherent control process, from weak field to strong field domains.

ACKNOWLEDGMENTS

This unnumbered section is used to identify those who have aided the authors in understanding or accomplishing the work presented and to acknowledge sources of funding.

REFERENCES

- [1] Neyra, E. G. and Vaveliuk, P., “Tailoring a sub-diffraction optical focus via a straightforward interferometric approach,” *Journal of Optics* **23**(7), 075604 (2021).
- [2] Diels, J.-C. and Rudolph, W., [*Ultrashort laser pulse phenomena*], Elsevier (2006).
- [3] Aharonov, Y., Colombo, F., Sabadini, I., Struppa, D., and Tollaksen, J., “Some mathematical properties of superoscillations,” *Journal of Physics A: Mathematical and Theoretical* **44**(36), 365304 (2011).
- [4] Berry, M., Zheludev, N., Aharonov, Y., Colombo, F., Sabadini, I., Struppa, D. C., Tollaksen, J., Rogers, E. T., Qin, F., Hong, M., et al., “Roadmap on superoscillations,” *Journal of Optics* **21**(5), 053002 (2019).
- [5] Gbur, G., “Using superoscillations for superresolved imaging and subwavelength focusing,” *Nanophotonics* **8**(2), 205–225 (2019).
- [6] Remez, R., Tsur, Y., Lu, P.-H., Tavabi, A. H., Dunin-Borkowski, R. E., and Arie, A., “Superoscillating electron wave functions with subdiffraction spots,” *Physical Review A* **95**(3), 031802 (2017).
- [7] Berry, M. and Popescu, S., “Evolution of quantum superoscillations and optical superresolution without evanescent waves,” *Journal of Physics A: Mathematical and General* **39**(22), 6965 (2006).
- [8] Shen, Y.-X., Peng, Y.-G., Cai, F., Huang, K., Zhao, D.-G., Qiu, C.-W., Zheng, H., and Zhu, X.-F., “Ultra-sonic super-oscillation wave-packets with an acoustic meta-lens,” *Nature communications* **10**(1), 1–7 (2019).
- [9] Zarkovsky, S., Ben-Ezra, Y., and Schwartz, M., “transmission of superoscillations,” *Scientific reports* **10**(1), 1–7 (2020).

- [10] Weiner, A. M., “Femtosecond pulse shaping using spatial light modulators,” *Review of scientific instruments* **71**(5), 1929–1960 (2000).
- [11] Boyko, O., Valentin, C., Rey, G., Antonucci, L., Balcou, P., and Coudreau, S., “Temporal superresolution of ultrashort laser pulses,” *Optics express* **13**(20), 8222–8230 (2005).
- [12] Binhammer, T., Rittweger, E., Morgner, U., Ell, R., and Kärtner, F., “Spectral phase control and temporal superresolution toward the single-cycle pulse,” *Optics letters* **31**(10), 1552–1554 (2006).
- [13] Eliezer, Y., Singh, B. K., Hareli, L., Arie, A., et al., “Experimental realization of structured super-oscillatory pulses,” *Optics express* **26**(4), 4933–4941 (2018).
- [14] Eliezer, Y., Hareli, L., Lobachinsky, L., Froim, S., and Bahabad, A., “Breaking the temporal resolution limit by superoscillating optical beats,” *Physical review letters* **119**(4), 043903 (2017).
- [15] Rausch, S., Binhammer, T., Harth, A., Kärtner, F. X., and Morgner, U., “Few-cycle femtosecond field synthesizer,” *Optics express* **16**(22), 17410–17419 (2008).
- [16] Keller, U., “Recent developments in compact ultrafast lasers,” *nature* **424**(6950), 831–838 (2003).
- [17] Goswami, D., “Optical pulse shaping approaches to coherent control,” *Physics Reports* **374**(6), 385–481 (2003).
- [18] Silberberg, Y., “Quantum coherent control for nonlinear spectroscopy and microscopy,” *Annual review of physical chemistry* **60**, 277–292 (2009).
- [19] Tanabe, T., Tanabe, H., Teramura, Y., and Kannari, F., “Spatiotemporal measurements based on spatial spectral interferometry for ultrashort optical pulses shaped by a fourier pulse shaper,” *JOSA B* **19**(11), 2795–2802 (2002).
- [20] Bardeen, C. J., Yakovlev, V. V., Squier, J. A., Wilson, K. R., Carpenter, S. D., and Weber, P. M., “Effect of pulse shape on the efficiency of multiphoton processes: implications for biological microscopy,” *Journal of Biomedical Optics* **4**(3), 362–367 (1999).
- [21] Sardesai, H., Chang, C.-C., and Weiner, A., “A femtosecond code-division multiple-access communication system test bed,” *Journal of Lightwave Technology* **16**(11), 1953 (1998).
- [22] Akturk, S., Kimmel, M., O’Shea, P., and Trebino, R., “Measuring pulse-front tilt in ultrashort pulses using grenouille,” *Optics Express* **11**(5), 491–501 (2003).
- [23] Neyra, E., Videla, F., Ciappina, M., Pérez-Hernández, J., Roso, L., and Torchia, G. A., “Synthesis of ultrashort laser pulses for high-order harmonic generation,” *Physical Review A* **98**(1), 013403 (2018).